The Electron Affinities of C_3O and C_4O

Jonathan C. Rienstra-Kiracofe,[†] G. Barney Ellison,[‡] Brian C. Hoffman,[†,§] and Henry F. Schaefer III*[,†]

Center for Computational Quantum Chemistry, University of Georgia, Athens, Georgia 30602-2525, and Department of Chemistry and Biochemistry, University of Colorado, Boulder, Colorado 80309-0215

Received: June 3, 1999; In Final Form: September 9, 1999

We predict the adiabatic electron affinities of C_3O and C_4O based on electronic structure calculations, using a large triple-ζ basis set with polarization and diffuse functions (TZ2Pf+diff) with the SCF, CCSD, and CCSD(T) methods as well as with the aug-cc-pVDZ and aug-cc-pVTZ basis sets. Our results imply electron affinities for C_3O and C_4O; EA(C_3O) = 0.93 eV ± 0.10 and EA(C_4O) = 2.99 ± 0.10. The EA(C_3O) is 0.41 eV lower than the experimental value of 1.34 ± 0.15 eV, while the EA(C_4O) is 0.94 eV higher than the experimental value of 2.05 ± 0.15 eV. Optimized geometries for all species at each level of theory are given, and harmonic vibrational frequencies are reported at the SCF/TZ2Pf+diff and CCSD/aug-cc-pVDZ levels.

1. Introduction

C_3O and C_4O are members of the important C_nO cluster family. Like the C_n series, members of the C_nO series are likely interstellar molecules.[1] Both C_3O (tricarbon monoxide) and C_4O have been studied by various experimental techniques. C_3O was first recognized by DeKock and Weltner in 1971 using matrix isolation IR spectroscopy.[2] Later, Berke and Härter demonstrated that C_3O can be an important ligand in inorganic compounds.[3] Gas-phase C_3O was first generated[4] in 1983, and subsequently C_3O was observed in interstellar space.[5] A mechanism for its interstellar production has been proposed.[6] Since these initial investigations, C_3O has been investigated using matrix-assisted IR,[7,8] microwave spectroscopy,[9−11] flash vacuum pyrolysis,[12] and Fourier transform IR spectroscopy.[13,14] Likewise, C_4O has been examined with electron spin resonance,[15] matrix isolation IR spectroscopy,[16] and Fourier transform microwave spectroscopy[17] but has not yet been observed in interstellar space. The C_4O^- anion has been observed using an RF ion trap;[18] otherwise, except for photoelectron experiment described next, there is no other experimental record of C_3O^- or C_4O^-.

In 1986, the photoelectron spectroscopy of the carbon oxide anions was studied.[19] The C_3O^- and C_4O^- ions were prepared by decomposition of carbon suboxide in a high-pressure electric discharge, and the 488-nm photodetachment spectra were studied: $C_nO^- + \hbar\omega_{488\ nm} \rightarrow C_nO + e^-$ ($n = 3, 4$). Since both anions were derived from an OC═C═CO discharge, the ions were assigned the structures $[CCCO]^-$ and $[CCCCO]^-$. Neither the photoelectron spectra of C_3O^- nor that of C_4O^- could be analyzed. The spectrum of C_3O^- featured a long 600 ± 35 cm^{-1} progression that disappeared into the noise at high kinetic energies. The first vibronic feature was chosen as the origin of the C_3O^- spectrum, with the EA(C_3O) assigned as 1.34 ± 0.15 eV. Due to the apparent large geometry change between the anion and the neutral species, this value should be regarded as an upper limit and more properly should be reported as EA(C_3O) ≤ 1.34 ± 0.15 eV. The spectrum of the C_4O^- was an unresolved continuum that extended over roughly 0.75 eV and was described as "essentially unanalyzable"; an EA(C_4O) was estimated as 2.05 ± 0.15 eV.

In the years since 1986, sophisticated theoretical methods have been developed that provide for accurate computation of molecular electron affinities. Theoretically, no examinations of the C_3O and C_4O electron affinities have been presented other than that of Kannari, et al., who predicted an electron affinity of 2.73 eV for C_4O at the CISD/[5s4p2d1f] ANO level.[20] Kannari et. al. concluded that a "remeasurement on the electron affinity of the C_4O molecule may be helpful". Recently, we have computed the electron affinity of C_4O with six density functionals: B3LYP, B3P86, BHLYP, BLYP, BP86, and LSDA, with a DZP++ basis.[21] These results all over-predict the experimental value by at least 0.74 eV (BLYP). In contrast, identical predictions with the same six functionals show close agreement to experiment (within 0.16 eV for all functionals except B3P86 and LSDA) for the EA(CCO).[22]

Previously, the electron affinity of BO was called into question by two of us,[23] and our high level CCSD(T)/aug-cc-pVQZ results suggested that the experimental value was wrong. Indeed, the EA(BO) was re-determined,[24] and the new photoelectron experimental value was found to be within 0.02 eV of our predicted EA. This close agreement demonstrates that high-level CCSD(T) results can closely agree with accurate methods such as photoelectron spectroscopy. On the basis of this previous success and the uncertain nature of the experimental EA's for C_3O and C_4O, we present here high-level ab initio predictions for the electron affinities of these species.

2. Theoretical Methods

Double- and triple-ζ basis sets with polarization and diffuse functions were employed in this study. Specifically, we employed the (10s6p/5s3p) contracted triple-ζ Gaussian functions of Dunning[25] augmented with two sets of *d* polarization functions and one set of f polarization functions. [$\alpha_d(C) = 1.50$ and 0.375, $\alpha_d(O) = 1.70$ and 0.425, $\alpha_f(C) = 0.80$ and $\alpha_f(O) = 1.40$] To complete the basis set, a set of diffuse s and p functions were added as determined by the "even-tempered" prescription

* To whom correspondence should be addressed.
[†] University of Georgia. E-mail: rienstra@ccqc.uga.edu.
[‡] University of Colorado. E-mail: barney@jila.colorado.edu.
[§] Present location: Department of Chemistry, Johns Hopkins University.

10.1021/jp9918104 CCC: $19.00
Published on Web 10/30/1999

of Lee and Schaefer.[26] [α_{s-diff}(C) = 0.04812, α_{s-diff}(O) = 0.08993, α_{p-diff}(C) = 0.03389, α_{p-diff}(O) = 0.05840] We refer to the total basis as TZ2Pf+diff, and it may be designated C,O-(11s7p2d1f/6s4p2d1f).

Additionally, the correlation-consistent polarized valence double- and triple-ζ (cc-pVDZ and cc-pVTZ) sets of Dunning[27] augmented with diffuse functions following Kendall et al.[28] (aug-cc-pVDZ and aug-cc-pVTZ) were employed. The aug-cc-pVDZ and aug-cc-pVTZ basis sets may be designated C,O(10s5p2d/4s3p2d) and C,O(11s6p3d2f/5s4p3d2f), respectively. Pure angular momentum functions (5d, 7f) were used in all cases.

Geometry optimizations were performed using analytic gradient techniques at the self-consistent field theory (SCF) and coupled cluster with single and double excitations (CCSD)[29−31] and CCSD with perturbative triple excitations (CCSD(T))[30,32,33] levels of theory. With the CCSD and CCSD(T) methods, all electrons were correlated, and no virtual orbitals were deleted. SCF harmonic vibrational frequencies were computed using analytic second derivatives and CCSD harmonic vibrational frequencies via finite differences of analytic first derivatives. A restricted open-shell Hartree−Fock reference was used. Molecular geometries were considered converged when the RMS gradient fell below 10^{-7} hartree/bohr. All computations were performed using the ACES II ab initio program system.[34]

Finally, analysis of C_4O and C_4O^- structural isomers was performed using density functional theory (DFT). Specifically, we employed the BP86 functional[35−37] with a DZP++ basis, which was constructed by augmenting the Huzinaga−Dunning set of contracted double-ζ Gaussian functions[38,39] with one set of d polarization functions [α_d (C) = 0.75, α_d (O) = 0.85] and a set of even-tempered s and p diffuse functions [α_{s-diff}(C) = 0.04302, α_{s-diff}(O) = 0.08227, α_{p-diff}(C) = 0.03629, α_{p-diff}(O) = 0.06508]. All DFT computations were performed in an identical manner as those in our previous C_4O EA results[21] and were obtained using GAUSSIAN 94.[40]

3. Results and Discussion

3.1. Bonding and Configurations. The carbon oxides show an interesting alternation in molecular properties.[41,42] The "even" oxides: C_2O, C_4O, C_6O, ... are all $\tilde{X}\ ^3\Sigma^-$ species, while the "odd" oxides: CO, C_3O, C_5O, ... are all $\tilde{X}\ ^1\Sigma^+$ molecules. The C_3O molecule can be represented[43] by the following expression:

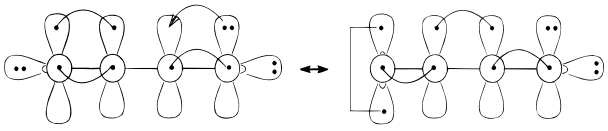

$\tilde{X}\ ^1\Sigma^+$ C-C-C-O

The dominant configuration that describes the ground state of C_3O is:

$$|\tilde{X}\ ^1\Sigma^+\rangle = [\text{core}]^8\ (5\sigma)^2(6\sigma)^2(7\sigma)^2(8\sigma)^2(1\pi)^4(9\sigma)^2(2\pi)^4 \quad (1)$$

The experimental microwave[9−11] and IR absorption[2,7,8,13,14] spectra of $\tilde{X}\ ^1\Sigma^+$ C_3O establish the ground geometry and four of the vibrational fundamentals. The experimental C_3O geometry [r_e(CCC≡O) = 1.150 Å, r_e(CC=CO) = 1.306 Å, r_e(C=CCO) = 1.254 Å][10] is consistent with the resonant configuration in eq 1. The unusually short C≡O bond is only slightly larger than carbon monoxide[44] and shorter than the C=O bonds in both formaldehyde and ketene. Both C=C bonds are slightly shorter than the C=C bond in ethylene but certainly longer than the C≡C of acetylene. From the above bonding picture and the experimental data, one can expect C_3O to exhibit polyacetylene-like bonding. As in carbon monoxide, we anticipate the first excited state of C_3O to be $\tilde{a}\ ^3\Pi$ and to be described as

$$|\tilde{a}\ ^3\Pi\rangle = [\text{core}]^8\ (5\sigma)^2(6\sigma)^2(7\sigma)^2(8\sigma)^2 \times (1\pi)^4(9\sigma)^1(2\pi)^4(3\pi)^1 \quad (2)$$

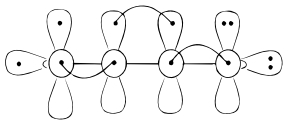

$\tilde{a}\ ^3\Pi$ C-C-C-O

Little is known about the C_3O^- anion, although we anticipate it to be an $\tilde{X}\ ^2\Pi$ state with the configuration:

$$|\tilde{X}\ ^2\Pi\rangle = [\text{core}]^8\ (5\sigma)^2(6\sigma)^2(7\sigma)^2(8\sigma)^2 \times (1\pi)^4(9\sigma)^2(2\pi)^4(3\pi)^1 \quad (3)$$

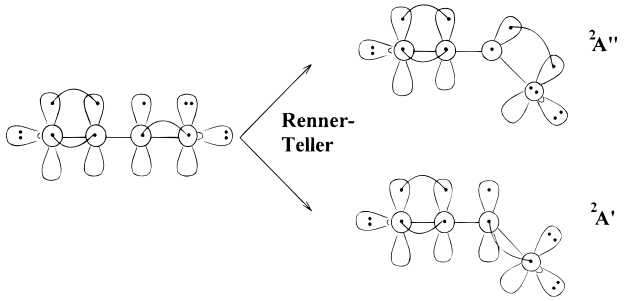

$\tilde{X}\ ^2\Pi$ C-C-C-O$^-$

The linear $^2\Pi$ species will distort into two Renner-Teller components. Bending in the "radical" plane alleviates the disfavorable interaction between the radical carbon and the oxygen lone pair while retaining favorable "allylic-like" C−C−C bonding. This $^2A'$ species will be lower in energy relative to the linear Π state. On the other hand, bending perpendicular to the "radical" plane does not alleviate the radical carbon−oxygen lone pair interaction and reduces any allylic-like bonding. This $^2A''$ species will be higher in energy than the $^2\Pi$ species. For closed-shell species such as CO and C_3O, the electron affinities are expected to be small. Since the EA(CO) is negative, we anticipate the EA(C_3O) to be small, and it is probably less than 1 eV.

Matrix isolated EPR and IR spectroscopy have established that C_4O and C_6O are triplet ground-state molecules.[15,16] We can describe the C_4O molecule as $\tilde{X}\ ^3\Sigma^-$:

$$|\tilde{X}\ ^3\Sigma^-\rangle = [\text{core}]^{10}\ (6\sigma)^2(7\sigma)^2(8\sigma)^2(9\sigma)^2(10\sigma)^2 \times (1\pi)^4(2\pi)^4(11\sigma)^2(3\pi)^2 \quad (4)$$

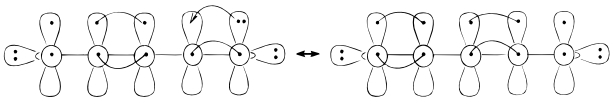

$\tilde{X}\ ^3\Sigma^-$ C-C-C-C-O

The $\tilde{X}\ ^3\Sigma^-$ configuration shows resonance between two structures with both unpaired electrons on either the C or O atoms; localization of the electron pair maximizes the pp' exchange integral, $K_{pp'}$, and minimizes the triplet energy. Although there are differences in eletronegativity between carbon and oxygen, one might expect an average structure which would exhibit a cumulene-like bonding. In addition to the ground

$\tilde{X}\ ^3\Sigma^-$ state, there will be a pair of low-lying $\tilde{a}\ ^1\Delta$ and $\tilde{b}\ ^1\Sigma^+$ electronic states also arising from the configuration given in eq 4; the $\tilde{a}\ ^1\Delta^-$ state is

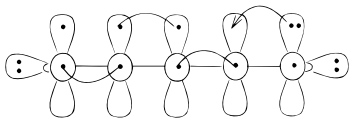

$\tilde{a}\ ^1\Delta^-$ C-C-C-C-O

The C_4O^- anion is likely to be $\tilde{X}\ ^2\Pi$ and will have as a dominant configuration

$$|\tilde{X}\ ^2\Pi\rangle = [\text{core}]^{10}\,(6\sigma)^2(7\sigma)^2(8\sigma)^2(9\sigma)^2(10\sigma)^2 \times (1\pi)^4(2\pi)^4(11\sigma)^2(3\pi)^3 \quad (5)$$

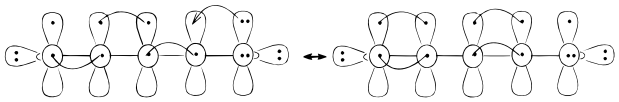

$\tilde{X}\ ^2\Pi$ C-C-C-C-O$^-$

Since $EA(C_2O) = 2.289 \pm 0.018$ eV,[45] it is likely that $EA(C_4O)$ will be greater than 2.5 eV. In addition to the $^2\Pi$ ground state, we anticipate that there will be a low-lying $^2\Sigma^+$ electronic state of C_4O^- which can be described as

$$|\tilde{A}\ ^2\Sigma^+\rangle = [\text{core}]^{10}\,(6\sigma)^2(7\sigma)^2(8\sigma)^2(9\sigma)^2(10\sigma)^2(11\sigma)^1 \times (1\pi)^4(2\pi)^4(3\pi)^4 \quad (6)$$

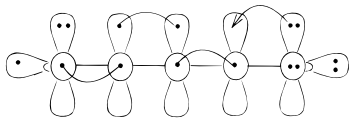

$\tilde{A}\ ^2\Sigma^+$ C-C-C-C-O$^-$

Two other excited configurations:

$$[\text{core}]^{10}\,(6\sigma)^2(7\sigma)^2(8\sigma)^2(9\sigma)^2(10\sigma)^2 \times (1\pi)^4(2\pi)^4(11\sigma)^2(3\pi)^2(4\pi)^1 \quad (7)$$

which, according to Hund's Rules, has a low-lying $^4\Pi$ state, and

$$[\text{core}]^{10}\,(6\sigma)^2(7\sigma)^2(8\sigma)^2(9\sigma)^2(10\sigma)^2 \times (1\pi)^4(2\pi)^4(11\sigma)^2(3\pi)^2(12\sigma)^1 \quad (8)$$

for which a low-lying $^4\Sigma^-$ state may also be anticipated.

3.2 Theoretical Results. Previous theoretical studies have predicted ground-state neutral C_3O to be linear with a $^1\Sigma^+$ ground state.[8,46−53] Indeed, harmonic vibrational frequencies determined with SCF,[46−47,51] CEPA,[48,49] and DFT (BLYP)[52] methods all predicted real harmonic frequencies for the linear structure. Similarly, earlier theoretical studies have predicted the most stable geometries of C_4O to be linear, with cumulene-like bonding in a $^3\Sigma^-$ electronic ground state.[20,21,52,54] Real harmonic frequencies were reported with the SCF,[54] MP2,[20] and DFT[21,52] methods. As mentioned previously, experimental studies of C_4O also support a linear, cumulene-like structure.[15,17] In Table 1 we report our optimized geometries for the $^1\Sigma^+$ C_3O and $^3\Sigma^-$ C_4O linear ground states.

Our SCF and BP86/DZP++ harmonic vibrational frequencies for both the $^1\Sigma^+$ C_3O and $^3\Sigma^-$ C_4O linear species are real and are shown in Table 2. On the other hand, CCSD/aug-cc-pVDZ harmonic frequencies show degenerate imaginary Π frequencies of 81*i* for C_3O and 234*i* for C_4O. Following the imaginary eigenvector for each leads to nonlinear, degenerate $^1A'$ C_3O structures and nonlinear, degenerate $^3A''$ C_4O structures which are 0.001 and 0.002 eV below $^1\Sigma^+$ C_3O and $^3\Sigma^-$ C_4O, respectively. These C_s stationary points are shown in Figure 1. It is not suprising that other methods (SCF, DFT, etc.), all of which include less electron correlation than CCSD, fail to characterize the linear C_3O and C_4O structures as transition states—the difference in energy between the linear and nonlinear structures is too small to be reliably obtained with a lower level of theory.

Although the above results suggest that C_3O and C_4O are nonlinear, they are essentially linear (or "floppy" molecules) nonetheless. Indeed, at the CCSD/aug-cc-pVDZ level the bond distances of the nonlinear structures are no more than 0.001 Å different than the linear structures. Furthermore, all angles are within 12 degrees of linearity. Botschwina had noted that the C−C−C bending potential in C_3O is "rather shallow".[49] Certainly, the potential energy surface about the angles in C_3O and C_4O is very flat in the linear region, as evidenced by the very small energy differences between the linear and nonlinear structures. Because energy differences of thousandths of an eV will not affect our theoretical electron affinity predictions, we discuss only the linear C_3O and C_4O species from this point on. However, the fact that neither C_3O or C_4O is rigidly linear may account for the large amounts of "noise" seen in the original photoelectron spectra.

For linear C_3O, at all levels of theory, we see a relatively short C−O bond which is consistent with the $\tilde{X}\ ^1\Sigma^+$ diagram 1. Furthermore, at the CCSD(T)/aug-cc-pVTZ level, the middle C−C bond is 0.025 Å longer than the terminus C−C bond. This alternation in bond length was expected, as discussed in the previous section. Furthermore, both the C−O and middle C−C bonds are within 0.009 Å of the experimental bond lengths of Brown et al.[10] However, the terminal C−C bond over-predicts experiment by 0.018 Å. It is worth mentioning that Brown et al. note that the center of mass condition was not fulfilled to their satisfaction in their substitution structure determination using Kraitchman's equations. In addition, if C_3O is not truly linear, a structure determination which assumes linearity would be slightly skewed. Indeed, their MP3/6-31G* bond length[46] was also too long, by 0.017 Å, in that instance. The work of both Tang et al.[9] and Brown et al.[10] gives a rotational constant (B_0) of 4810.9 MHz. Our CCSD(T)/aug-cc-pVTZ geometry corresponds to a B_e of 4793.0 MHz, which is in reasonable agreement with the experimental value. Moreover, comparing our ab initio results to those of Botschwina and Reisenauer,[8] who combined experimental ground-state rotational constants and theoretical vibration−rotation coupling constants to obtain a B_0 of 4801.0 MHz, yields even better agreement. In fact, Botschwina and Reisenauer suggest a geometry (which they believe is accurate to within 0.0005 Å) of $r_e(CCC{\equiv}O) = 1.1473$ Å, $r_e(CC{=}CO) = 1.2965$ Å, $r_e(C{=}CCO) = 1.2717$ Å, which is within 0.003 Å of our best results for all three bond lengths. This excellent agreement demonstrates that the CCSD(T)/aug-cc-pVTZ method describes the C_3O system well.

For linear C_4O, one notes that the middle C−C bonds are nearly identical in length, with the terminal C−C bond being roughly 0.03 Å longer. All three C−C bonds are longer than the triple bond in acetylene but shorter than the double bond in ethylene.[44] The C−O bond is 0.013 Å longer than the C−O bond in C_3O and approximately the same length as that of

TABLE 1: Optimized Geometries for C_3O ($\tilde{X}\ ^1\Sigma^+$), C_3O^- ($\tilde{X}\ ^2\Pi$), C_3O^- ($\tilde{X}\ ^2A'$), C_4O ($\tilde{X}\ ^3\Sigma^+$), C_4O^- ($\tilde{X}\ ^2\Pi$), and C_4O^- ($\tilde{A}\ ^2\Sigma^+$)[a]

method/basis	r_1	r_2	r_3	θ_1	θ_2
		C_3O ($\tilde{X}\ ^1\Sigma^+$)			
SCF/aug-cc-pVDZ	1.124	1.302	1.260	–	–
SCF/TZ2Pf+diff	1.117	1.293	1.247	–	–
SCF/aug-cc-pVTZ	1.118	1.294	1.248	–	–
BP86/DZP++ (ref 58)	1.176	1.316	1.301	–	–
CCSD/aug-cc-pVDZ	1.155	1.318	1.288	–	–
CCSD/TZ2Pf+diff	1.140	1.297	1.264	–	–
CCSD/aug-cc-pVTZ	1.139	1.294	1.261	–	–
CCSD(T)/aug-cc-pVDZ	1.165	1.320	1.299	–	–
CCSD(T)/TZ2Pf+diff	1.151	1.299	1.275	–	–
CCSD(T)/aug-cc-pVTZ	1.150	1.297	1.272	–	–
expt (ref 10)	1.150	1.306	1.254	–	–
		C_3O^- ($\tilde{X}\ ^2\Pi$)			
SCF/aug-cc-pVDZ	1.189	1.271	1.316	–	–
SCF/TZ2Pf+diff	1.180	1.262	1.303	–	–
SCF/aug-cc-pVTZ	1.182	1.262	1.303	–	–
CCSD/aug-cc-pVDZ	1.217	1.310	1.320	–	–
CCSD/TZ2Pf+diff	1.202	1.289	1.295	–	–
CCSD/aug-cc-pVTZ	1.200	1.287	1.292	–	–
CCSD(T)/aug-cc-pVDZ	1.225	1.318	1.327	–	–
CCSD(T)/TZ2Pf+diff	1.209	1.296	1.302	–	–
CCSD(T)/aug-cc-pVTZ	1.208	1.294	1.300	–	–
		C_3O^- ($\tilde{X}\ ^2A'$)			
SCF/aug-cc-pVDZ[b]	–	–		–	–
SCF/TZ2Pf+diff[b]	–	–	–	–	–
SCF/aug-cc-pVTZ[b]	–	–	–	–	–
BP86/DZP++ (ref 58)	1.235	1.378	1.295	148.4	166.4
CCSD/aug-cc-pVDZ	1.216	1.399	1.280	138.9	164.9
CCSD/TZ2Pf+diff	1.201	1.376	1.255	139.7	167.5
CCSD/aug-cc-pVTZ	1.200	1.368	1.254	140.6	169.3
CCSD(T)/aug-cc-pVDZ	1.225	1.398	1.292	139.1	163.4
CCSD(T)/TZ2Pf+diff	1.211	1.375	1.266	139.9	166.3
CCSD(T)/aug-cc-pVTZ	1.210	1.366	1.265	141.0	168.3

method/basis	r_1	r_2	r_3	r_4
		C_4O ($\tilde{X}\ ^3\Sigma^-$)		
SCF/aug-cc-pVDZ	1.134	1.288	1.269	1.320
SCF/TZ2Pf+diff	1.127	1.280	1.259	1.308
BP86/DZP++ (ref 21)	1.190	1.304	1.308	1.337
CCSD/aug-cc-pVDZ	1.168	1.304	1.298	1.330
CCSD/TZ2Pf+diff	1.154	1.284	1.278	1.306
CCSD(T)/aug-cc-pVDZ	1.178	1.308	1.306	1.336
CCSD(T)/TZ2Pf+diff	1.164	1.288	1.286	1.312
		C_4O^- ($\tilde{X}\ ^2\Pi$)		
SCF/aug-cc-pVDZ	1.185	1.249	1.337	1.269
SCF/TZ2Pf+diff	1.177	1.240	1.328	1.256
BP86/DZP++ (ref 21)	1.229	1.281	1.351	1.304
CCSD/aug-cc-pVDZ	1.215	1.275	1.353	1.294
CCSD/TZ2Pf+diff	1.200	1.254	1.334	1.269
CCSD(T)/aug-cc-pVDZ	1.222	1.283	1.355	1.303
CCSD(T)/TZ2Pf+diff	1.208	1.261	1.335	1.278
		C_4O^- ($\tilde{A}\ ^2\Sigma^+$)		
SCF/aug-cc-pVDZ	1.201	1.232	1.371	1.209
SCF/TZ2Pf+diff	1.193	1.222	1.363	1.198
CCSD/aug-cc-pVDZ	1.228	1.259	1.376	1.248
CCSD/TZ2Pf+diff	1.213	1.238	1.357	1.225
CCSD(T)/aug-cc-pVDZ	1.234	1.269	1.373	1.259
CCSD(T)/TZ2Pf+diff	1.219	1.247	1.354	1.236

[a] All bond lengths are in Å, r_1 refers to the C−O bond, and each successive r_n refers to a C−C bond starting from the oxygen terminus. For C_3O^- ($\tilde{X}\ ^2A'$), θ_1 is the O−C−C angle and θ_2 is the C−C−C angle with an O−C−C−C torsion angle of 180 degrees. [b] Not a minimum at this level.

carbon dioxide.[44] These results are in accordance with a cumulene-like bonding picture, as shown in diagram 4.

Both the C_3O and C_4O anions are $^2\Pi$ ground states. Kannari et al. studied two geometric structures for C_4O^-: a linear structure and a bent "V"-shaped structure.[20] They concluded that the linear structure was the global minimum, with the bent structure being less stable by about 4 kcal mol^{-1}. Although they obtain a single imaginary frequency of 67*i* at the MP2 level for the linear species, they report no stationary point corresponding to this mode. Our results for geometry optimizations of the linear C_3O^- and C_4O^- anions are presented in Table 1. The linear structures of both anions possess a $^2\Pi$ electronic state, which can be expected to suffer from the Renner-Teller effect.[55,56] Analysis of the Π-type vibrational bending modes with our previous six DFT results[21] and the current SCF harmonic frequencies (see Table 2) show that C_4O^- is a "case A" Renner-Teller[57] molecule with respect to all sets of bending modes; that is, all three doubly degenerate Π harmonic vibrational

TABLE 2: Harmonic Vibrational Frequencies at the SCF/TZ2Pf+diff, BP86/DZP++, and CCSD/aug-cc-pVDZ Levels[a]

		C_3O ($\tilde{X}\ ^1\Sigma^+$)			C_3O^- ($\tilde{X}\ ^2\Pi$)			C_3O^- ($\tilde{X}\ ^2A'$)		
mode	symmetry	SCF	BP86[c]	CCSD	SCF	BP86	CCSD	SCF[b]	BP86[c,d]	CCSD[c]
ω_1	Π_a	121	139	81*i*	193	370*i*	366*i*	–	212	163
ω_2	Π_b	121	139	81*i*	288	192	125	–	216	224
ω_3	Π_b	688	551	592	391	251	240	–	498	554
ω_4	Π_a	688	551	592	711	561	589	–	885	911
ω_5	Σ^+	1031	915	956	993	876	914	–	1686	1770
ω_6	Σ^+	2151	1867	1972	1513	1561	1585	–	1857	1952
ω_6	Σ^+	2470	2259	2321	2145	2046	2047	–	–	–
ZPVE		10.4	9.2	9.2	8.9	7.8	7.9	–	8.0	8.0

		C_4O ($\tilde{X}\ ^3\Sigma^-$)			C_4O^- ($\tilde{X}\ ^2\Pi$)			C_4O^- ($\tilde{A}\ ^2\Sigma^+$)
mode	symmetry	SCF	BP86	CCSD	SCF	BP86	CCSD	SCF
ω_1	Π_a	105	121	234*i*	129	143	261*i*	92
ω_2	Π_b	105	121	234*i*	142	87	175*i*	92
ω_3	Π_b	461	298	141	468	358	182	660
ω_4	Π_a	461	298	141	488	336	152	660
ω_5	Π_a	646	444	500	594	492	453	754
ω_6	Π_b	646	444	500	683	420	527	754
ω_7	Σ^+	827	737	769	803	721	745	788
ω_8	Σ^+	1502	1390	1454	1578	1398	1452	1591
ω_9	Σ^+	2136	1891	1990	2037	1852	1921	2311
ω_{10}	Σ^+	2447	2224	2307	2395	2186	2266	2380
ZPVE		13.4	11.2	11.2	13.3	11.4	11.0	14.4

[a] All values are in cm^{-1}. Zero point vibrational energies (ZPVE) are in kcal mol^{-1}. Note: Π_a normal modes represent bending in the plane of the SOMO, and Π_b normal modes represent bending perpendicular to the SOMO plane ($^2\Pi$ states only). [b] Not a minimum at this level. [c] ω_1 is A″ symmetry all others are A′. [d] Reference 58.

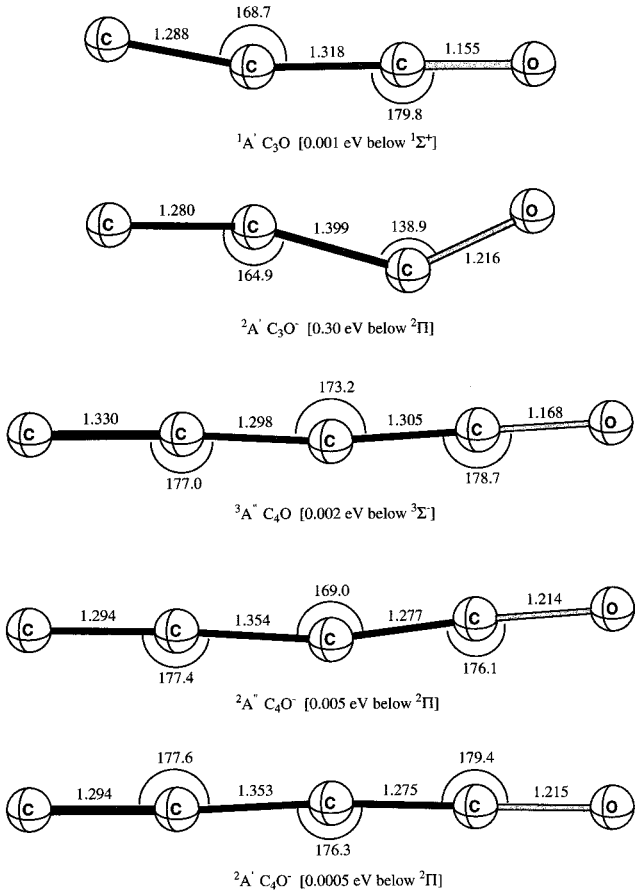

Figure 1. Nonlinear C_s structures of C_3O, C_3O^-, C_4O, and C_4O^-. All values are from CCSD/aug-cc-pVDZ.

modes are split into distinct, real frequencies. On the other hand, CCSD/aug-cc-pVDZ frequencies suggest C_4O^- is a "case D" Renner-Teller[57] molecule; that is, it has two attractive bending potentials, leading to two distinct nonlinear structures of lower energy that result from different imaginary harmonic frequencies (261*i* and 175*i*). Likewise, although SCF suggests C_3O^- is linear, both BP86/DZP++ and CCSD/aug-cc-pVDZ results agree that C_3O^- is a "case C" Renner-Teller[57] molecule; that is, it has one atractive bending potential, leading to a nonlinear structure of lower energy that results from a single imaginary frequency (ca. 370*i*). (See diagram 3.)

The two nonlinear structures of C_4O^- ($^2A'$ and $^2A''$) are shown in Figure 1. As in the case of the parent neutral, both structures are essentially linear and lie just 0.005 ($^2A''$) and 0.0005 ($^2A'$) eV below the linear $^2\Pi$ state. The bond distances of each nonlinear structure are within 0.002 Å of the linear distances, and all angles are within 11 degrees of linearity—indicating that C_4O^- is essentially linear. Again, the energy differences between the two nonlinear structures and the linear structure are extremely small and likely impossible to be detected with SCF and current DFT functionals. As with C_4O, we chose only to study the linear C_4O^- structure with higher levels of theory. Nonetheless, both Renner-Teller components will be populated in a mass-selected beam. Detachment of such a population will lead to a congested C_4O^- photoelectron spectrum.[19]

Examining linear C_4O^-, we observe a very sharp decrease over the parent neutral in bond lengths r_2 and r_4 and a correspondingly large increase in lengths of the r_3 and C−O (r_1) bonds. Again, the changes were anticipated, as seen from diagram 5 in section 3.1, namely, that the additional electron partially destroys the cumulene-like bonding observed in C_4O. Such changes in geometry between the neutral and anion are significant as they often are noticed in photoelectron spectra.

The C_3O^- species does have a significantly bent minimum ($^2A'$) that is about 0.2−0.3 eV below the linear $^2\Pi$ state (See Figure 1). This difference is large enough to be detected by BP86/DZP++ (other functionals likewise agree[58]) but is still overlooked at the SCF level. Table 1 gives the optimized geometry for $^2A'$ C_3O^-, which is significantly different than $^2\Pi$ C_3O^-. The C−O bond (r_1) is nearly identical in length to that in the linear structure; however, the middle C−C bond (r_2) increases by about 0.08 Å, and the terminal C−C bond (r_3)

TABLE 3: Ab Initio Predictions for the Adiabatic Detachment Energies of C_3O and C_4O[a]

method/basis	neutral energy	anion energy	detachment energy
	C_3O ($\tilde{X}\ ^1\Sigma^+$)	C_3O^- ($\tilde{X}\ ^2\Pi$)	
SCF/aug-cc-pVDZ	−188.35200	−188.35559	0.10
SCF/TZ2Pf+diff	−188.40071	−188.40122	0.01
SCF/aug-cc-pVTZ	−188.39658	−188.39744	0.02
CCSD/aug-cc-pVDZ	−188.91794	−188.94477	0.73
CCSD/TZ2Pf+diff	−189.11363	−189.13883	0.69
CCSD/aug-cc-pVTZ	−189.11672	−189.14423	0.75
CCSD(T)/aug-cc-pVDZ	−188.95260	−188.97779	0.69
CCSD(T)/TZ2Pf+diff	−189.15550	−189.17920	0.64
CCSD(T)/aug-cc-pVTZ	−189.16039	−189.18705	0.73
	C_3O ($\tilde{X}\ ^1\Sigma^+$)	C_3O^- ($\tilde{X}\ ^2A'$)	
BP86/DZP++ (ref 58)	−189.42553	−189.47246	1.28
CCSD/aug-cc-pVDZ	−188.91794	−188.95593	1.03
CCSD/TZ2Pf+diff	−189.11363	−189.14828	0.94
CCSD/aug-cc-pVTZ	−189.11672	−189.15252	0.97
CCSD(T)/aug-cc-pVDZ	−188.95260	−188.98834	0.97
CCSD(T)/TZ2Pf+diff	−189.15550	−189.18808	0.89
CCSD(T)/aug-cc-pVTZ	−189.16039	−189.19467	0.93
	C_4O ($\tilde{X}\ ^3\Sigma^-$)	C_4O^- ($\tilde{X}\ ^2\Pi$)	
SCF/aug-cc-pVDZ	−226.14166	−226.21910	2.11
SCF/TZ2Pf+diff	−226.19862	−226.27521	2.08
BP86/DZP++ (ref 21)	−227.45951	−227.56924	2.99
CCSD/aug-cc-pVDZ	−226.83045	−226.93462	2.83
CCSD/TZ2Pf+diff	−227.06784	−227.17351	2.88
CCSD(T)/aug-cc-pVDZ	−226.87034	−226.97546	2.86
CCSD(T)/TZ2Pf+diff	−227.11699	−227.22357	2.90
CCSD(T)/aug-cc-pVTZ//CCSD(T)/TZ2Pf+diff	−227.12375	−227.23350	2.99
	C_4O ($\tilde{X}\ ^3\Sigma^-$)	C_4O^- ($\tilde{A}\ ^2\Sigma^+$)	
SCF/aug-cc-pVDZ	−226.14166	−226.17026	0.78
SCF/TZ2Pf+diff	−226.19862	−226.22821	0.81
CCSD/aug-cc-pVDZ	−226.83045	−226.88131	1.38
CCSD/TZ2Pf+diff	−227.06784	−227.12205	1.48
CCSD(T)/aug-cc-pVDZ	−226.87034	−226.92127	1.39
CCSD(T)/TZ2Pf+diff	−227.11699	−227.17115	1.47
CCSD(T)/aug-cc-pVTZ//CCSD(T)/TZ2Pf+diff	−227.12375	−227.18133	1.57

[a] Total energies are given in hartrees and detachment energies in eV. Note that the reported values are not zero-point corrected.

decreases by about 0.04 Å. The O−C−C angle (θ_1) is strongly bent (about 140 degrees) in the opposite direction of the less bent C−C−C angle (θ_2); that is, the $^2A'$ C_3O^- is in a "trans" configuration. Certainly, these geometry changes are consistent with the original photoelectron spectrum.

The electronic configuration of the C_4O^- ($^2\Pi$) anion was given in eq 5. The first excited state represents promotion of an electron from the 11σ orbital to the 3π orbital. This gives an excited $^2\Sigma^+$ state with the electronic configuration given in eq 6. Our best result places this state at 1.42 eV higher than the ground $^2\Pi$ state. In addition to the $^2\Sigma^+$ state, we investigated both quartet states of the configurations given in eqs 7 and 8. A stability analysis performed at the SCF level and an EOM-CCSD/aug-cc-pVDZ examination at the C_4O^- ($^2\Pi$) geometry revealed no other excited states below 2.83 eV (the detachment threshold). Thus, it is not surprising that at the SCF/TZ2Pf+diff and CCSD/aug-cc-pVDZ levels we were unable to locate a bound structure for the $^4\Sigma^-$ state. The C_4O^- ($^4\Pi$) state is 2.68 eV (SCF) and 3.01 eV (CCSD) above the $^2\Pi$ ground state, which is above the predicted detachment threshold at both levels of theory. Nonetheless, we observed an imaginary frequency of 795*i* at the SCF level—indicating the presence of a bent Renner-Teller species. Such a species was indeed located and is a minimum with an O−C_1−C_2 angle of about 130 degrees and essentially linear C_2−C_3−C_4 bonds using CCSD/aug-cc-pVDZ. This C_s ($^2A''$) species is 0.94 and 1.11 eV lower than the $^4\Sigma$ state at the SCF/TZ2Pf+diff and CCSD/aug-cc-pVDZ levels, respectively. No further examinations of this state were performed, as it is too high in energy relative to C_4O^- ($^2\Pi$) to account for the 2.05 eV feature observed by Oakes and Ellison. Nonetheless, the presence of the linear $^2\Sigma^+$ and the bent $^2A''$ states below the detachment threshold is significant, as most anions do not have any bound excited states. One might expect similar excited states for other members of the C_nO^- ($n > 4$, n is even) family.

The results of our predicted adiabatic electron affinities for C_3O and C_4O (reported in Table 3) converge upon definite values. We find EA(C_3O) = 0.93 and EA(C_4O) = 2.99 eV. The estimated error of ±0.10 eV accounts for both inadaquacies in the level of theory and the fact that linear species of C_3O, C_4O, and C_4O^- are not truly linear. The C_3O value is 0.41 eV lower than the experimental value and is consistent with the large geometry change in the original spectrum. The C_4O results are similar to our previous DFT work[21] on C_4O, which reported a BP86/DZP++ EA of 2.99 eV. As may be expected, the SCF results, which lack electron correlation, differ greatly from the higher-correlated levels of theory, and the C_4O SCF results are deceptively close to the experimental value. As may be evidenced from the zero-point vibrational energies given in Table 2, zero-point corrections to the predicted electron affinities should be minimal at best. Finally, the adiabatic detachment potential of the first excited state of C_4O^- appears to converge upon a value of 1.57 ± 0.10 eV. This value is 0.48 eV lower than the reported experimental value for the electron affinity of C_4O. Thus it appears that the C_4O^- $\tilde{A}\ ^2\Sigma^+$ excited state was not active in the experiments of Oakes and Ellison.[19]

Despite both experimental and theoretical evidence that both C_4O and C_4O^- are linear or nearly so and that C_4O is a ground-state triplet, the inconsistency between the experimental photoelectron spectrum[19] and our hitherto discussed theoretical

TABLE 4: Ab Initio Predictions for the Adiabatic Electron Affinites (in eV) of Various Structural C_4O and C_4O^- Isomers[a]

isomer/method	neutral (energy)	ΔE	anion (energy)	ΔE	EA (eV)
linear					
BP86/DZP++ (ref 21)	−227.45951	0.0	−227.56924	0.0	2.99
CISD//MP2/DZP	−226.85805	0.0	−226.95848	0.0	2.73
"diamond"-shaped					
BP86/DZP++	−227.43624	14.5	–	–	–
CISD//MP2/DZP	−226.83904	12.0	–	–	–
"V"-shaped					
BP86/DZP++	–	–	–	–	–
CISD//MP2/DZP	−226.83601	13.8	−226.94903	6.0	3.08
"T"-shaped					
BP86/DZP++	−227.42797	19.8	−227.52834	25.6	2.73
CISD//MP2/DZP	−226.82995	17.5	–	–	–

[a] Total energies are given in hartrees, relative energies in kcal mol^{-1}. CISD//MP2/DZP results are from ref 20. See Figure 2 for optimized geometries of the "T"-shaped and "diamond"-shaped isomers and Figure 3b for a pictorial representation of this table.

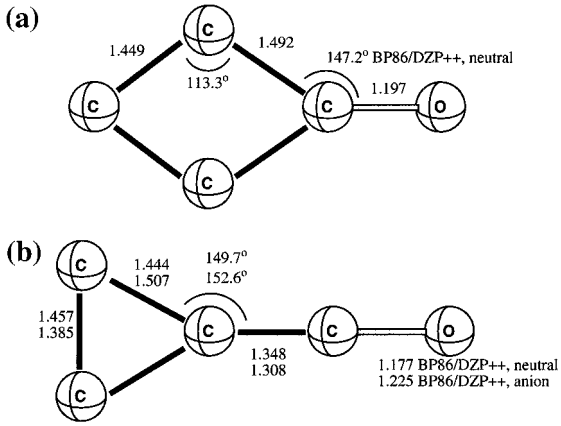

Figure 2. BP86/DZP++ optimized geometries of structural isomers of C_4O/C_4O^-. All distances are in angstroms and bond angles in degrees. (a) "Diamond"-shaped structure [C_4O, $^1A_1$], and (b) "T"-shaped structure [C_4O, $^1A_1$; C_4O^-, $^2B_1$].

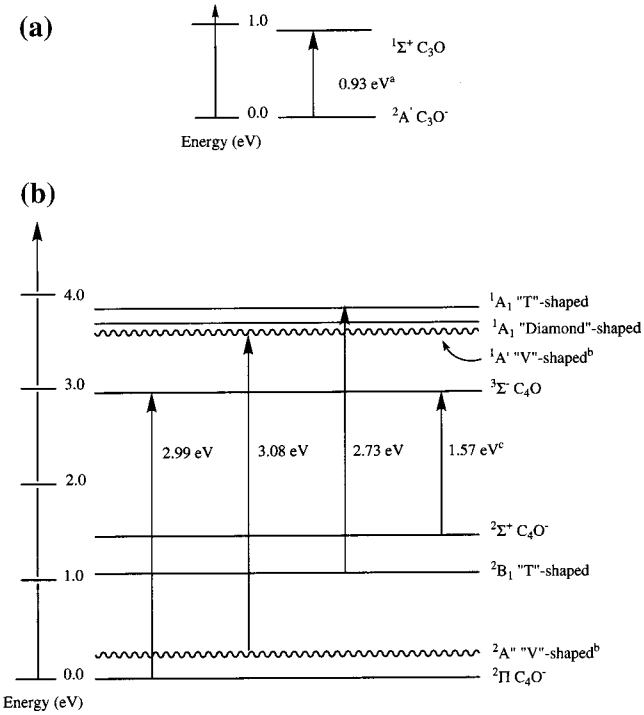

Figure 3. Detachment energies (eV) for C_3O^- (a) and various C_4O^- moieties (b). All values are at the BP86/DZP++ level, except [a]CCSD(T)/aug-cc-pVTZ, [b]CISD//MP2/DZP (ref 20), and [c]CCSD(T)/aug-cc-pVTZ//CCSD(T)/TZ2Pf+diff.

results prompted us to consider whether any structural isomers of C_4O and C_4O^- may account for the observed EA of 2.05 eV. As mentioned earlier, Kannari et al. concluded that the linear C_4O and C_4O^- structures were each the global minimum on their respective potential energy surfaces, with an electron affinity of 2.73 eV at the CISD//MP2/DZP level.[20] They also reported a bent "V"-shaped isomer for both the anion and neutral species, which gave an electron affinity of 3.08 eV. While Kannari et al. did locate two other structural isomers of neutral C_4O, they failed to find corresponding C_4O^- structural isomers.

Having already examined the linear isomers using the BP86/DZP++ level of theory[21] (See Tables 1 and 3), we explored the isomeric structures first examined by Kannari et al. Our DFT optimizations of both the neutral and anion "V"-shaped structures led to the linear isomers in both instances. It seems unclear whether these isomers exist at all or rather if they are not minima on the BP86/DZP++ potential energy surface. Nonetheless, the results of Kannari et al. show that they could not account for the experimentally observed EA.

Besides the "V"-shaped structure, and in agreement with Kannari et al., we located a "diamond"-shaped isomer (See Figure 2a) for the neutral species only. We also located the "T"-shaped structure that Kannari et al. reported for neutral C_4O. Additionally, we were able to find the corresponding "T"-shaped anion isomer (Figure 2b). The "T"-shaped isomers may result from the perpendicular addition of C_2 (or C_2- for the anion) to CCO. The BP86/DZP++ results suggest an electron affinity of 2.73 eV for this isomer.

Our DFT results, together with those of Kannari et al., are summarized in Table 4 and shown in Figure 3b. Note that each structural isomer is less stable than the linear structure and that all isomers (including the linear species) yield electron affinities greater than the laser photon energy (2.540 eV) used in the original experiment. While it may be possible that an excited state in the "V"- or "T"-shaped anion could account for the observed spectrum, the likelihood of such a bizarre occurrence being observed physically seems minute.

4. Conclusion

Our findings are strong evidence that the reported value for the electron affinity of C_3O (1.34 ± 0.15 eV) is somewhat high. The more likely value for EA(C_3O) is 0.93 ± 0.10 eV, and this is consistent with the experimental spectrum.[19]

The experimental photoelectron spectrum[19] of C_4O^- contains a feature at electron kinetic energy 0.49 ± 0.15 eV which translates into an effective binding energy of 2.05 ± 0.15 eV. But our computational result for the electron affinity of C_4O is 2.99 ± 0.10 eV, which is not compatible with a binding energy of 2.05 eV. A 488 nm laser will not be able to photodetach

such a strongly bound anion because the photon energy (2.540 eV) is less than the electron binding energy, $\hbar\omega_{488} < EA(C_4O) \simeq 3$ eV. One way out of this dilemma would be that the C_4O^- ion beam produced by the C_3O_2 high pressure electric discharge contained a population of electronically excited C_4O^- anions, $\tilde{A}\ ^2\Sigma^+\ C_4O^-$. If the term value for this species were roughly $T_e(\tilde{A}\ ^2\Sigma^+\ C_4O^-) = 0.94$ eV, detachment of these metastable anions could be the source of the observed photoelectrons: $\tilde{A}\ ^2\Sigma^+\ C_4O^- + \hbar\omega_{488} \rightarrow {}^3\Sigma^-\ C_4O + e^-$, since [2.99−0.94 = 2.05 eV]. However, our estimated term value for $\tilde{A}\ ^2\Sigma^+\ C_4O^-$ is 1.42 eV, and this is not consistent with this interpretation. Furthermore, although analysis of structural C_4O/C_4O^- isomers suggest "T"-shaped and (perhaps) bent "V"-shaped isomers, both are less stable than the linear structure and also correspond to electron affinities greater than the laser detachment threshold. These, then, are likewise inconsistent the original spectrum.

Certainly, our results presented here imply that the electron affinity of C_4O is incorrect. However, a satisfactory explanation of the 2.05 eV feature observed in the photoelectron experiment has not been found. In the past 13 years, new ion sources have been developed, and the resolution of the electrostatic analyzers has improved by an order of magnitude. Consequently the negative ion photoelectron spectrum shoud be revisited: $C_4O^- + \hbar\omega_{351\ nm} \rightarrow C_4O + e^-$. These experimental efforts may require more extensive theoretical explorations of the C_4O/C_4O^- potential energy surfaces.

Acknowledgment. The authors thank Dr. G. S. Tschumper for sharing DFT results, which first indicated that C_3O^- is bent. The research of J.C.R.-K. and H.F.S. was supported by the U.S. Department of Energy, Office of Basic Energy Sciences, Division of Chemical Sciences, Fundamental Interaction Branch, Grant No. DE-FG02-97-ER14748. J.C.R.-K. thanks Christine Rienstra-Kiracofe for research assistance. G.B.E. is supported by a grant from the Chemical Physics Program, U.S. Department of Energy (DE-FG02-87ER13695). This paper is a tribute to Prof. Bill Goddard on the occasion of his 60th birthday. For many years, we have admired his originality and style in the study of Valence. From Athens and Boulder, we salute the Captain of the Weenie Diagrams! G.B.E. and H.F.S. were privileged to attend the Pasadena birthday party, including the lavish banquet at Burger Continental.

References and Notes

(1) Adams, N. G.; Smith, D.; Giles, K.; Herbst, E. *Astron. Astrophys.* **1989**, *220*, 269.
(2) DeKock, R. L.; Weltner, W., Jr. *J. Am. Chem. Soc.* **1971**, *93*, 7106.
(3) Berke, H.; Härter, P. *Angew. Chem., Int. Ed. Engl.* **1980**, *19*, 225.
(4) Brown, R. D.; Eastwood, F. W.; Elmes, P. S.; Godfrey, P. D. *J. Am. Chem. Soc.* **1983**, *105*, 6496.
(5) Matthews, H. E.; Irvine, W. M.; Friberg, P.; Brown, R. D.; Godfrey, P. D. *Nature* **1984**, *310*, 125.
(6) Herbst, E.; Smith, D.; Adams, N. G. *Astron. Astrophys.* **1984**, *138*, L13.
(7) Brown, R. D.; Pullin, D. E.; Rice, E. H. N.; Rodler, M. *J. Am. Chem. Soc.* **1985**, *107*, 7877.
(8) Botschwina, P.; Reisenauer, H. P. *Chem. Phys. Lett.* **1991**, *183*, 217.
(9) Tang, T. B.; Inokuchi, H.; Saito, S.; Yamada, C.; Hirota, E. *Chem. Phys. Lett.* **1985**, *116*, 83.
(10) Brown, R. D.; Godfrey, P. D.; Elmes, P. S.; Rodler, M.; Tack, L. M. *J. Am. Chem. Soc.* **1985**, *107*, 4112.
(11) Brown, R. D. *Int. Rev. Phys. Chem.* **1986**, *5*, 101.
(12) Brown, R. F. C.; Godfrey, P. D.; Lee, S. C. *Tetrahedron Lett.* **1985**, *26*, 6373.
(13) McNaughton, D.; McGilvery, D.; Shanks, F. *J. Mol. Spectrosc.* **1991**, *149*, 458.
(14) Szczepanski, J.; Ekern, S.; Vala, M. *J. Phys. Chem.* **1995**, *99*, 8002.
(15) Van Zee, R. J.; Smith, G. R.; Weltner, W., Jr. *J. Am. Chem. Soc.* **1988**, *110*, 609.
(16) Maier, G.; Reisenauer, H. P.; Schäfer, U.; Balli, H. *Angew. Chem., Int. Ed. Engl.* **1988**, *27*, 566.
(17) Ohshima, Y.; Endo, Y.; Ogata, T. *J. Chem. Phys.* **1995**, *102*, 1493.
(18) Watanabe, N.; Shiromaru, H.; Negishi, Y.; Achiba, Y.; Kobayashi, N.; Kaneko, Y. *Z. Phys. D* **1993**, *26*, S252.
(19) Oakes, J. M.; Ellison, G. B. *Tetrahedron* **1986**, *42*, 6263.
(20) Kannari, H.; Aoki, K.; Hashimoto, K.; Ikuta, S. *Chem. Phys. Lett.* **1994**, *222*, 313.
(21) Brown, S. T.; Rienstra-Kiracofe, J. C.; Schaefer, H. F. *J. Phys. Chem.* **1999**, *103*, 4065.
(22) Tschumper, G. S.; Schaefer, H. F. *J. Chem. Phys.* **1997**, *107*, 2529.
(23) Rienstra, J. C.; Schaefer, H. F. *J. Chem. Phys.* **1997**, *106*, 8278.
(24) Wenthold, P. G.; Kim, J. B.; Jonas, K.; Lineberger, W. C. *J. Phys. Chem. A* **1997**, *101*, 4472.
(25) Dunning T. H., Jr. *J. Chem. Phys.* **1971**, *55*, 716.
(26) Lee, T. J.; Schaefer, H. F. *J. Chem. Phys.* **1985**, *83*, 1784.
(27) Dunning, T. H. Jr. *J. Chem. Phys.* **1989**, *90*, 1007.
(28) Kendall, R. A.; Dunning, T. H.; Harrison, R. J. *J. Chem. Phys.* **1992**, *96*, 6796.
(29) Purvis, G. D.; Bartlett, R. J. *J. Chem. Phys.* **1982**, *76*, 1910.
(30) Rittby, M.; Bartlett, R. J. *J. Phys. Chem.* **1988**, *92*, 3033.
(31) Gauss, J.; Lauderdale, W. J.; Stanton, J. F.; Watts, J. D.; Bartlett, R. J. *Chem. Phys. Lett.* **1991**, *182*, 207.
(32) Watts, J. D.; Gauss, J.; Bartlett, R. J. *Chem. Phys. Lett.* **1992**, *200*, 1.
(33) Watts, J. D.; Gauss, J.; Bartlett, R. J. *J. Chem. Phys.* **1993**, *98*, 8718.
(34) Stanton, J. F.; Gauss, J.; Watts, J. D.; Nooijen, M.; Oliphant, N.; Perera, S. A.; Szalay, P. G.; Lauderdale, W. J.; Gwaltney, S. R.; Beck, S.; Balkova, A.; Bernholdt, D. E.; Baeck, K. K.; Rozyczko, P.; Sekino, H.; Hober, C.; Bartlett, R. J. *ACES II*, a program product of the Quantum Theory Project, University of Florida. Integral packages included are *VMOL* (Almlöf, J.; Taylor, P. R.); *VPROPS* (Taylor, P.); *ABACUS* (Helgaker, T.; Jensen, H. J. A.; Jörgensen, P.; Olsen, J.; Taylor, P. R.).
(35) Becke, A. D. *Phys. Rev. A* **1988**, *38*, 3098.
(36) Perdew, J. P. *Phys. Rev. B* **1986**, *33*, 8822.
(37) Perdew, J. P. *Phys. Rev. B* **1986**, *34*, 7406.
(38) Huzinaga, S. *J. Chem. Phys.* **1965**, *42*, 1293.
(39) Dunning, T. H., Jr. *J. Chem. Phys.* **1970**, *53*, 2823.
(40) Frisch, M. J.; Trucks, G. W.; Schlegel, H. B.; Gill, P. M. W.; Johnson, B. G.; Robb, M. A.; Cheeseman, J. R.; Keith, T.; Petersson, G. A.; Montgomery, J. A.; Raghavachari, K.; Al-Laham, M. A.; Zakrzewski, V. G.; Ortiz, J. V.; Foresman, J. B.; Cioslowski, J.; Stefanov, B. B.; Nanayakkara, A.; Challacombe, M.; Peng, C. Y.; Ayala, P. Y.; Chen, W.; Wong, M. W.; Andres, J. L.; Replogle, E. S.; Gomperts, R.; Martin, R. L.; Fox, D. J.; Binkley, J. S.; Defrees, D. J.; Baker, J.; Stewart, J. P.; Head-Gordon, M.; Gonzalez, C.; Pople, J. A. *GAUSSIAN 94*, Revision C.3; Gaussian, Inc.: Pittsburgh, PA, 1995.
(41) Jacox, M. E. *Vibrational and Electronic Energy Levels of Polyatomic Transient Molecules*; American Institue of Physics: Woodbury, NY, 1994; p 11797.
(42) Jacox, M. E. *J. Phys. Chem. Ref. Data* **1998**, *27*, 115.
(43) Goddard, W. A., III; Harding, L. B. *Annu. Rev. Phys. Chem.* **1978**, *29*, 363.
(44) Harmony, M. D.; Laurie, V. W.; Kuczkowski, R. J.; Schwendeman, R. H.; Ramsay, D. A.; Lovas, F. J.; Lafferty, W. J.; Maki, A. G. *J. Phys. Chem. Ref. Data* **1979**, *8*, 619−712. It is helpful to know the experimental bond lengths for some carbon/oxygen bonds: $r_e(CO) = 1.128$ Å, $r_e(OC{=}O) = 1.162$ Å, $r_e(H_2C{=}O) = 1.206$ Å, $r_e(H_2C{=}CO) = 1.314$ Å, $r_e(H_2CC{=}O) = 1.161$ Å, $r_e(H_3C{-}OH) = 1.425$ Å, $r_e(HC{\equiv}CH) = 1.207$ Å, $r_e(H_2C{=}CH_2) = 1.339$ Å, $r_e(H_3C{-}CH_3) = 1.512$ Å.
(45) Zengin, V.; Persson, B. J.; Strong, K. M.; Continetti, R. E. *J. Chem. Phys.* **1996**, *105*, 9740.
(46) Brown, R. D.; Rice, E. H. N. *J. Am. Chem. Soc.* **1984**, *106*, 6475.
(47) Brown, R. D.; McNaughton, D.; Dyall, K. G. *Chem. Phys.* **1988**, *119*, 189.
(48) Botschwina, P. *J. Chem. Soc., Faraday Trans. 2* **1988**, *84*, 1263.
(49) Botschwina, P. *J. Chem. Phys.* **1989**, *90*, 4301.
(50) Janoschek, R. *THEOCHEM* **1991**, *232*, 147.
(51) Maclagan, R. G. A. R.; Sudkeaw, P. *J. Chem. Soc., Faraday Trans.* **1993**, *89*, 3325.
(52) Moazzen-Ahmadi, N.; Zerbetto, F. *J. Chem. Phys.* **1995**, *103*, 6343.
(53) Ekern, S.; Vala, M. *J. Phys. Chem. A* **1997**, *101*, 3601.
(54) Ewing, D. W. *J. Am. Chem. Soc.* **1989**, *111*, 8809.
(55) Herzberg, G.; Teller, E. *Z. Phys. Chem. B* **1933**, *21*, 410.
(56) Renner, R. *Z. Phys.* **1934**, *92*, 172.
(57) Lee, T. J.; Fox, D. J.; Schaefer, H. F.; Pitzer, R. M. *J. Chem. Phys.* **1984**, *81*, 356.
(58) Tschumper, G. S.; Brown, S. T.; Barden, C. J.; Schaefer, H. F. work in progress, 1999.